Eur. Phys. J. C 18, 181–193 (2000)
Digital Object Identifier (DOI) 10.1007/s100520000520

THE EUROPEAN PHYSICAL JOURNAL C

The $\gamma\gamma \to A^0A^0$ process at a $\gamma\gamma$ collider*

G.J. Gounaris, P.I. Porfyriadis

Department of Theoretical Physics, Aristotle University of Thessaloniki, 54006, Thessaloniki, Greece

Received: 12 July 2000 / Published online: 13 November 2000 – © Springer-Verlag 2000

Abstract. The helicity amplitudes for the process $\gamma\gamma \to A^0A^0$ are studied to 1-loop order in the minimal SUSY (MSSM) model, where A^0 is the CP-odd Higgs particle. Simple exact analytic formulae are obtained in terms of the C_0 and D_0 Passarino–Veltman functions, in spite of the fact that the loop diagrams often involve different particles running along their sides. For a usual mSUGRA set of parameters, $\sigma(\gamma\gamma \to A^0A^0) \sim 0.1$–$0.2\,\mathrm{fb}$ is expected. If SUSY is realized in nature, these expressions should be useful for understanding the Higgs sector.

1 Introduction

If in the future e^-e^+ linear colliders (LCs) [1] the option to develop high energy $\gamma\gamma$ collisions will also be available, then many new opportunities for new physics (NP) searches should arise. Employing back-scattering of laser photons, this option transforms an[1] LC to essentially a $\gamma\gamma$ collider ($\mathrm{LC}_{\gamma\gamma}$) with about 80% of the initial energy and a comparable luminosity [2,3]. The importance of $\mathrm{LC}_{\gamma\gamma}$ stems from the fact that the cross sections for gauge boson and top production in $\gamma\gamma$ collisions at sufficiently high energies are often considerably larger than the corresponding quantities in the e^-e^+ case [4,5].

To some extent, such an enhancement should arise for Higgs production also. For the neutral Higgs particles in particular, an $\mathrm{LC}_{\gamma\gamma}$ may act as a Higgs factory which can be used to study their properties in detail, including possible Higgs anomalous couplings [6,7]. Since the anomalous gauge boson, top and Higgs couplings are interconnected and constitute an important possible source of new physics, an $\mathrm{LC}_{\gamma\gamma}$ should be very helpful for its identification. In case the NP scale is very high, such forms of NP may be described by the complete list of dim = 6 operators involving gauge bosons and/or quarks of the third family presented in [8].

Alternatively, it may turn out that the NP scale is close at hand, as would be expected in the usual SUSY scenario [9]. In such a case many neutral spinless particles of Higgs and sneutrino type may exist, and an $\mathrm{LC}_{\gamma\gamma}$ may be used for s-channel production of the CP-even light and heavy neutral Higgs bosons h^0 and H^0, respectively, as well as the CP-odd A^0. The study of the various branching ratios and the polarization of the incoming photons could then be very helpful to establish and disentangle the nature of these Higgs particles [11,12].

Once any of these spinless bosons is discovered, its properties should be carefully looked at, in order to be sure that they fulfill the SUSY expectations. Motivated by this, we study in this paper the process $\gamma\gamma \to A^0A^0$ in the context of a minimal SUSY model where no new sources of CP-violation, apart from those already known in the standard model (SM) Yukawa potential, are assumed to exist. Thus, the various new SUSY couplings are taken to be real, but no specific assumption on their relative magnitudes or signs is made [10]. As we will see below, in such a case, there are only two independent helicity amplitudes for $\gamma\gamma \to A^0A^0$, denoted below as F_{++} and F_{+-}, where the indices describe the helicities of the incoming photons.

It is also interesting to study the phases of these amplitudes. The motivation for this stems from the recent observation in [13,14] that at c.m. energies $\gtrsim 250\,\mathrm{GeV}$, out of the many independent helicity amplitudes for the processes $\gamma\gamma \to \gamma\gamma, \gamma Z, ZZ$, only the two helicity conserving amplitudes F_{++++} and F_{+-+-} are important, which moreover turn out to be almost purely imaginary[2]. The physical reason for this result is not very clear [13,14]. Therefore, it seems worthwhile to investigate what happens in other processes, like e.g. the neutral Higgs boson production, which, as neutral gauge boson production, also vanish at tree order and first appear at the 1-loop level.

Below, in Sect. 2, we give an overall view of the $\gamma\gamma \to A^0A^0$ helicity amplitudes in SUSY. The needed SUSY vertices appear in Appendix A, while the corresponding contributions to the amplitudes are given in Appendix B. The results are expressed in terms of the C_0 and D_0 Passarino–Veltman functions only [15], using expressions analogous

* Partially supported by the European Community grant ERBFMRX-CT96-0090.

[1] In this case it would be best to run LC in its e^-e^- mode [2,3]

[2] For $\gamma\gamma \to ZZ$ in SM the further assumption is made that the standard Higgs particle is light; e.g. below $\sim 200\,\mathrm{GeV}$

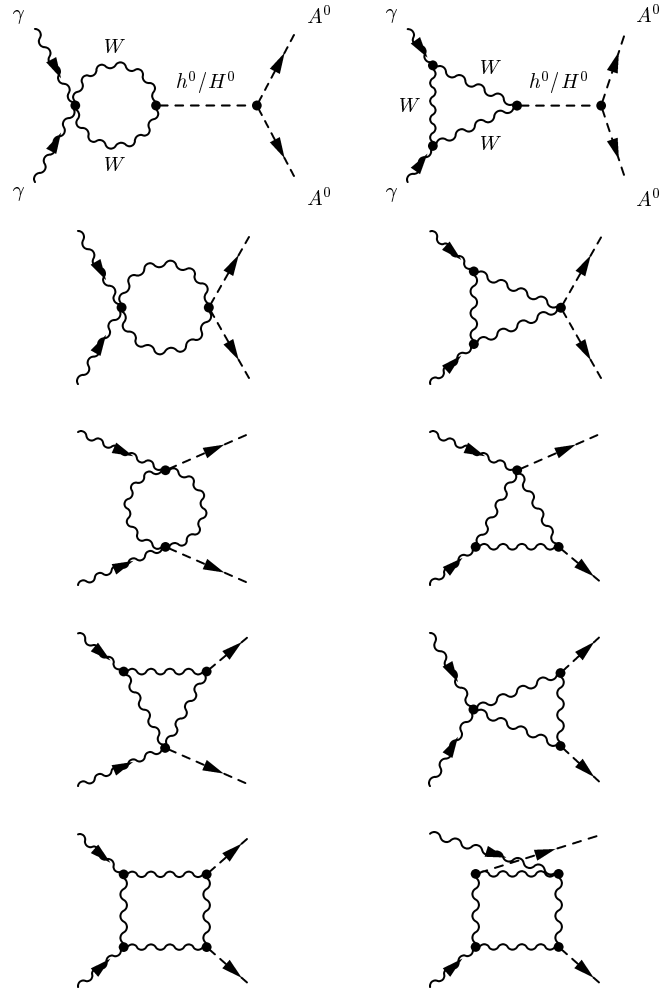

Fig. 1. Diagrams describing the $(W^{\pm}, H^{\pm})$ loop contribution to $\gamma\gamma \to A^0A^0$ in SUSY models. The internal wavy lines describe either a $W^{\pm}$ propagator (together with the associated Goldstone and ghost ones) or an $H^{\pm}$ one

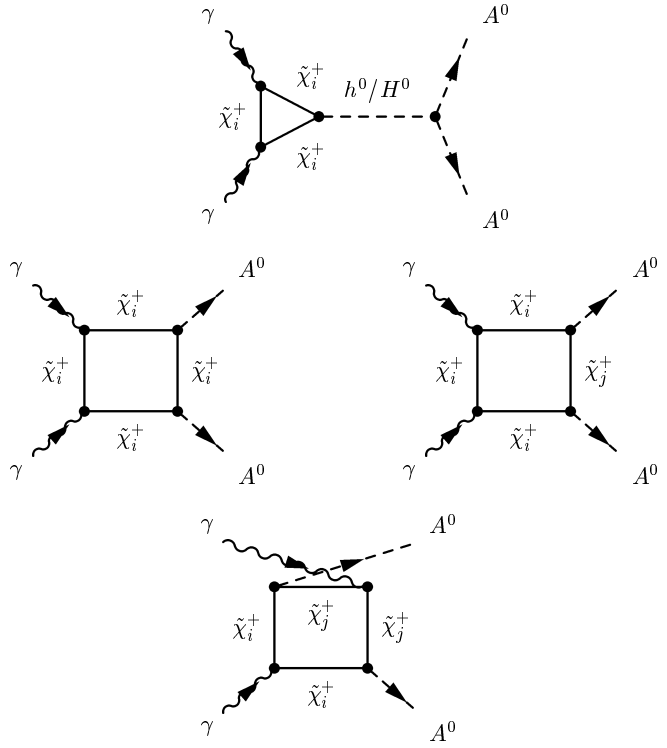

Fig. 2. Diagrams describing the chargino contributions to the $\gamma\gamma \to A^0A^0$ in SUSY models. The last three boxes may involve both $\tilde{\chi}_1$ ($\equiv \tilde{\chi}_1^+$) and $\tilde{\chi}_2$, running simultaneously along the loop

to those encountered in the $\gamma\gamma \to ZZ$ calculation [14]. Finally, in Sect. 3, we give our conclusions.

Turning now to the related studies already existing in the literature, we first remark that $\gamma\gamma \to h^0h^0$ has been studied in SM by Jikia [16]. In the non-linear gauge defined in (A.1) and used here, the only contributing diagrams involve W or top loops, similar to those appearing in Figs. 1 and 3. We have repeated the calculations of [16] and agree with the results, apart from the overall sign of the[3] F_{++} amplitude. For the top contributions, our results are fully consistent with those of [17]. The relevant amplitudes are presented and compared to those of $\gamma\gamma \to A^0A^0$ at the end of Sect. 2.

In [20] a calculation of $\gamma\gamma \to h^0h^0$ in a general SUSY model has been presented in terms of the general C_j and D_j Passarino–Veltman functions. The production of two neutral Higgs pairs in SUSY models at hadronic colliders has also been studied in [21], where of course the complications from loops involving W-bosons, or "single" and "mixed" charginos, are avoided. Finally, the processes $\gamma\gamma \to H^0H^0$ and $\gamma\gamma \to A^0A^0$ have also appeared in a non-supersymmetric gauge model involving a two Higgs doublet scalar sector [22,23].

2 An overall view of the $\gamma\gamma \to A^0A^0$ amplitudes

The invariant helicity amplitudes for[4] $\gamma\gamma \to A^0A^0$ are denoted by $F_{\lambda_1,\lambda_2}(\hat{s},\hat{t},\hat{u})$, where the λ_j describe the helicities of the incoming photons, and the kinematics are defined in Appendix B. Assuming that the SUSY Higgs potential is CP-invariant, we get (see (B.2))

$$F_{\lambda_1,\lambda_2}(\hat{s},\hat{t},\hat{u}) = F_{-\lambda_1,-\lambda_2}(\hat{s},\hat{t},\hat{u}), \tag{1}$$

which implies that there are only two independent helicity amplitudes, $F_{++}(\hat{s},\hat{t},\hat{u})$ and $F_{+-}(\hat{s},\hat{t},\hat{u})$.

As in [13,14], we employ the non-linear gauge of [24], which implies the gauge fixing and FP-ghost interactions of (A.1) and (A.2), leading to the conclusion that there are no $\gamma W^{\pm}G^{\mp}$, $ZW^{\pm}G^{\mp}$ vertices. The diagrams contributing to A^0-pair production are then given in Figs. 1–4.

[3] For the gauge boson polarization vectors, here and in [13, 14], we use the same conventions as in [18]. The only difference is that we use the JW convention [19], which introduces an additional minus to the polarization vector of a longitudinal "Number 2" Z and affects $\gamma\gamma \to ZZ, \gamma Z$

[4] We use the same conventions as in [13,14]

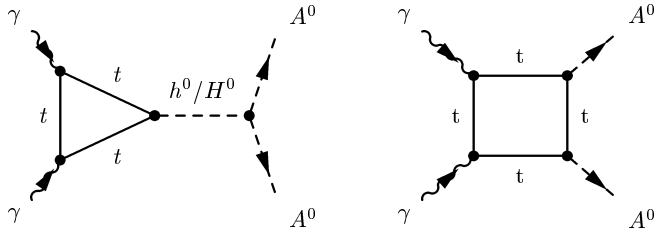

Fig. 3. Diagrams describing the top contributions to $\gamma\gamma \to A^0A^0$ in SUSY models. Similarly for the b-quark loop

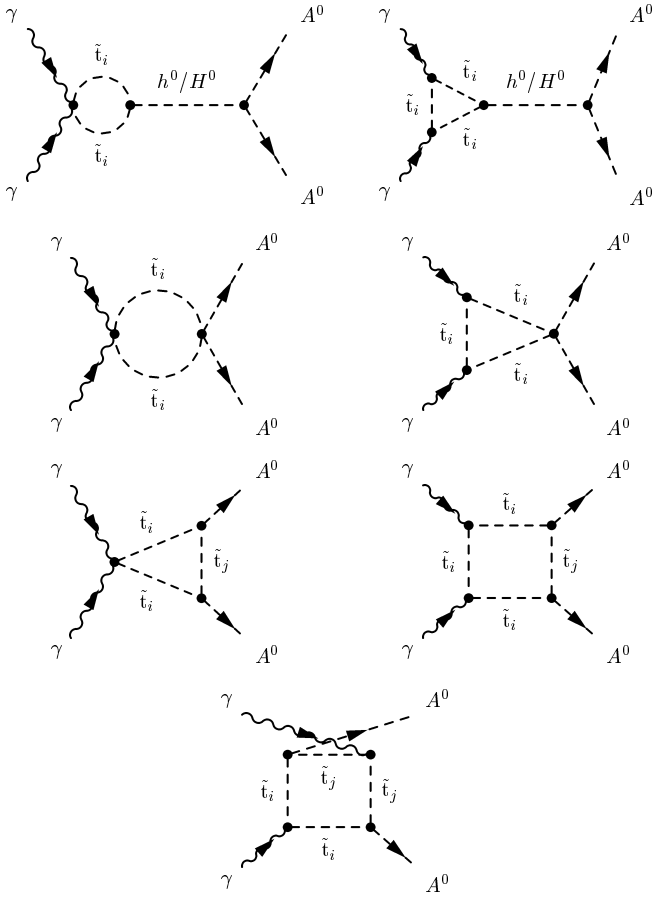

Fig. 4. The stop contributions to $\gamma\gamma \to A^0A^0$ in SUSY models. The last three diagrams may involve both $\tilde{t}_1$ and $\tilde{t}_2$ running simultaneously along the loop

Table 1. mSUGRA parameters in Figs. 5–7 [25]

	mSUGRA(1)	mSUGRA(2) (light stop)	mSUGRA(3)
$\tan\beta$	3	30	3
	at the Unification scale		
m_0 (GeV)	100	160	100
$M_{1/2}$ (GeV)	200	200	200
A_0 (GeV)	0	600	-715
sign (μ)	+	+	+
	at the Electroweak scale		
M_2 (GeV)	152	150	153
μ (GeV)	316	263	435
m_{A^0} (GeV)	375	257	489
m_{h^0} (GeV)	97.7	108	101
m_{H^0} (GeV)	379	257	490
$m_{H^\pm}$ (GeV)	383	269	495
A_t (GeV)	-373	-258	-500
$m_{\tilde{\chi}_1^+}$ (GeV)	128	132	138
$m_{\tilde{\chi}_2^+}$ (GeV)	346	295	454
$m_{\tilde{t}_1}$ (GeV)	295.4	353	133
$m_{\tilde{t}_2}$ (GeV)	494.2	469	491

The contribution to the F_{++} and F_{+-} amplitudes from the diagrams in Fig. 1 consists of two types. The first one is induced by the two diagrams in the first line in Fig. 1 and describes the (h^0, H^0)-pole contributions appearing in (B.19) and (B.20). The diagrams in the second to last line of Fig. 1 involve loops in which $W^\pm$ and/or $H^\pm$ are running along their internal lines. These induce the second type of contributions contained in (B.22) and (B.23) and expressed in terms of the (C_0, D_0) functions explained in (B.8)–(B.14), as well as the functions $\tilde{F}^{WH^\pm}$, $\tilde{F}^{H^\pm W}$, $E_1^{WH^\pm}$ defined in (B.15) and (B.16). The contributions (B.22) and (B.23) give the largest effect to the $\gamma\gamma \to A^0A^0$ amplitudes for the numerical applications considered below.

The chargino loop contribution is described by the diagrams in Fig. 2. It consists also of an (h^0, H^0)-pole contribution given in (B.24), the box contributions involving a "single chargino"-loop giving (B.26) and (B.27), and the "mixed chargino" contribution (B.28) and (B.29), arising when both charginos are running along the loop. Analytically, the later is the most complicated one. Nevertheless, it is simple enough to be possible to write it. Numerically, it has to be taken into account only when both charginos are relatively light.

The t- and b-quark contributions are described by the diagrams in Fig. 3. They are given in (B.31) for the (h^0, H^0)-pole contribution, and in (B.33) and (B.34) for the box diagrams.

As an example of a sfermion contribution, we only considered the one arising from the $(\tilde{t}_1, \tilde{t}_2)$-loop, described by the diagrams in Fig. 4. Their contributions are given by (B.35)–(B.38).

For the numerical applications we use the three CP-invariant mSUGRA set of parameters introduced in [25, 10] and presented in Table 1. For the electromagnetic coupling we take $\alpha = 1/127.8$. The results are shown in Figs. 5–7.

The real and imaginary parts of the helicity amplitudes $F_{++}(\gamma\gamma \to A^0A^0)$ and F_{+-} are presented in Figs. 5–7 [26]. As indicated there, the most important contributions to the amplitudes arise from the $(W, H^\pm)$-loop diagrams presented in the 2nd to last line of Fig. 1 and appearing in (B.22) and (B.23). At sufficiently high energies, these con-

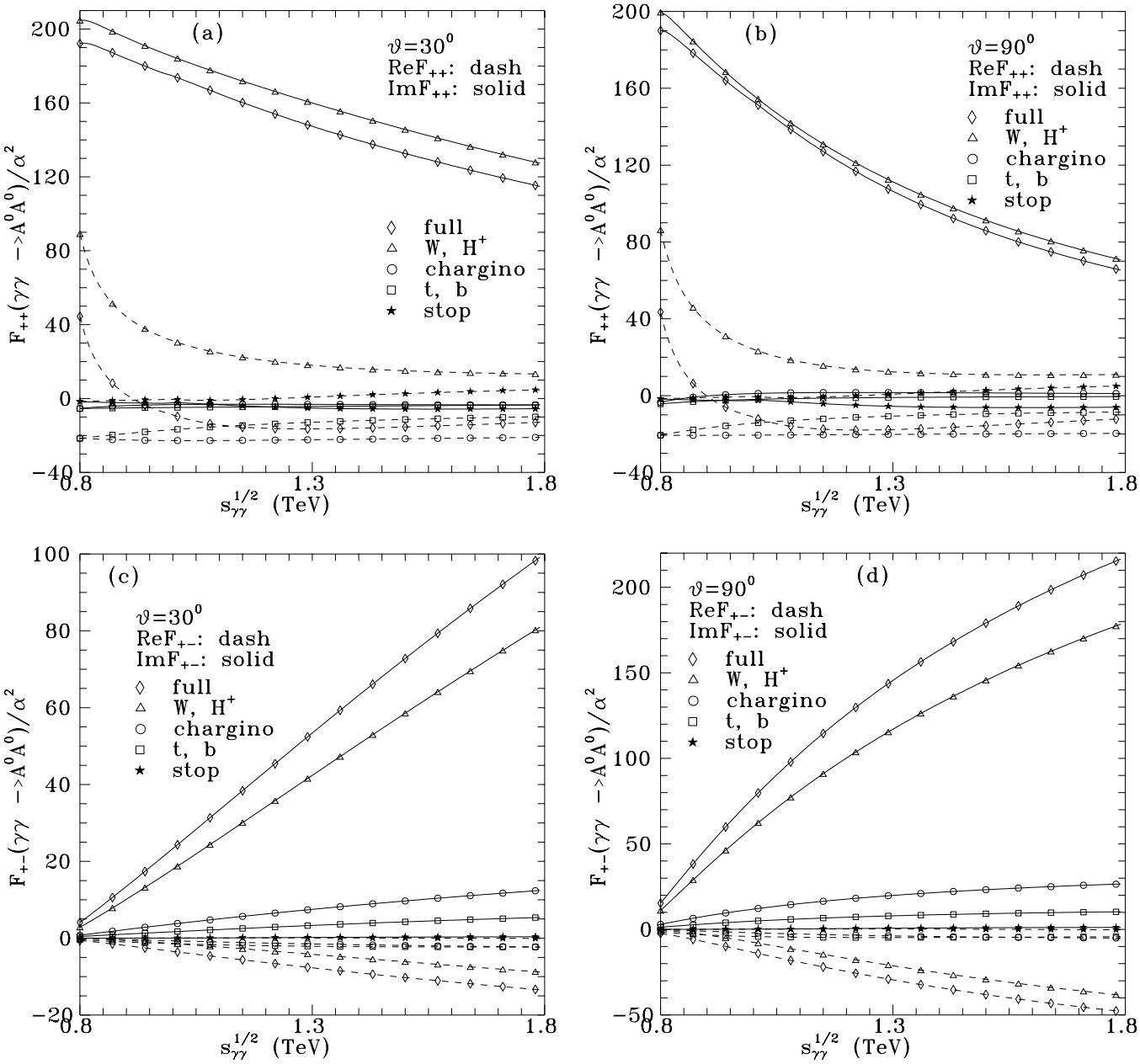

Fig. 5a–d. $\gamma\gamma \to A^0A^0$ helicity amplitudes as functions of the $\gamma\gamma$ center-of-mass energy $s_{\gamma\gamma} \equiv \hat{s}$ for mSUGRA(1); see Table 1

tributions are mainly imaginary. But the predominance of the imaginary parts of the amplitudes is not so strong as the one observed in the gauge boson production cases [13, 14].

As indicated in Figs. 5–7, the chargino contribution is generally quite important; while the t, b-quark contribution is somewhat smaller; and the stop contribution is negligible for the above cases.

For the t, b-quark contribution we also remark that in the mSUGRA(1) and mSUGRA(3) cases, where $\tan\beta$ is small, the b contribution is negligible compared to the top one. On the contrary, for the mSUGRA(2) case of $\tan\beta = 30$, the b-quark contribution may be more important than the t-quark one.

For comparison, we have also looked at the F_{++} and F_{+-} amplitudes for $\gamma\gamma \to h^0h^0$ in the standard model. The results for $m_{h^0} = 120\,\text{GeV}$ are given in Fig. 8. For the F_{++} we find that the *top*-loop contributions are comparable to the W ones, and the amplitude is never particularly imaginary. It is only for F_{+-}, for which there is no Higgs-pole contribution, that at energies $\gtrsim 600\,\text{GeV}$, the W-loop is more important than the top one, and the imaginary part of the amplitude becomes predominant.

The $\gamma\gamma \to A^0A^0$ unpolarized cross sections for the sets of parameters in Table 1 are given in Fig. 9. It lies in the range of ~ 0.1–$0.2)$ fb, which is similar but somewhat smaller than the result expected for $\sigma(\gamma\gamma \to h^0h^0)$ in SM for $m_{h^0} \sim 120\,\text{GeV}$ [16]. This result does not seem par-

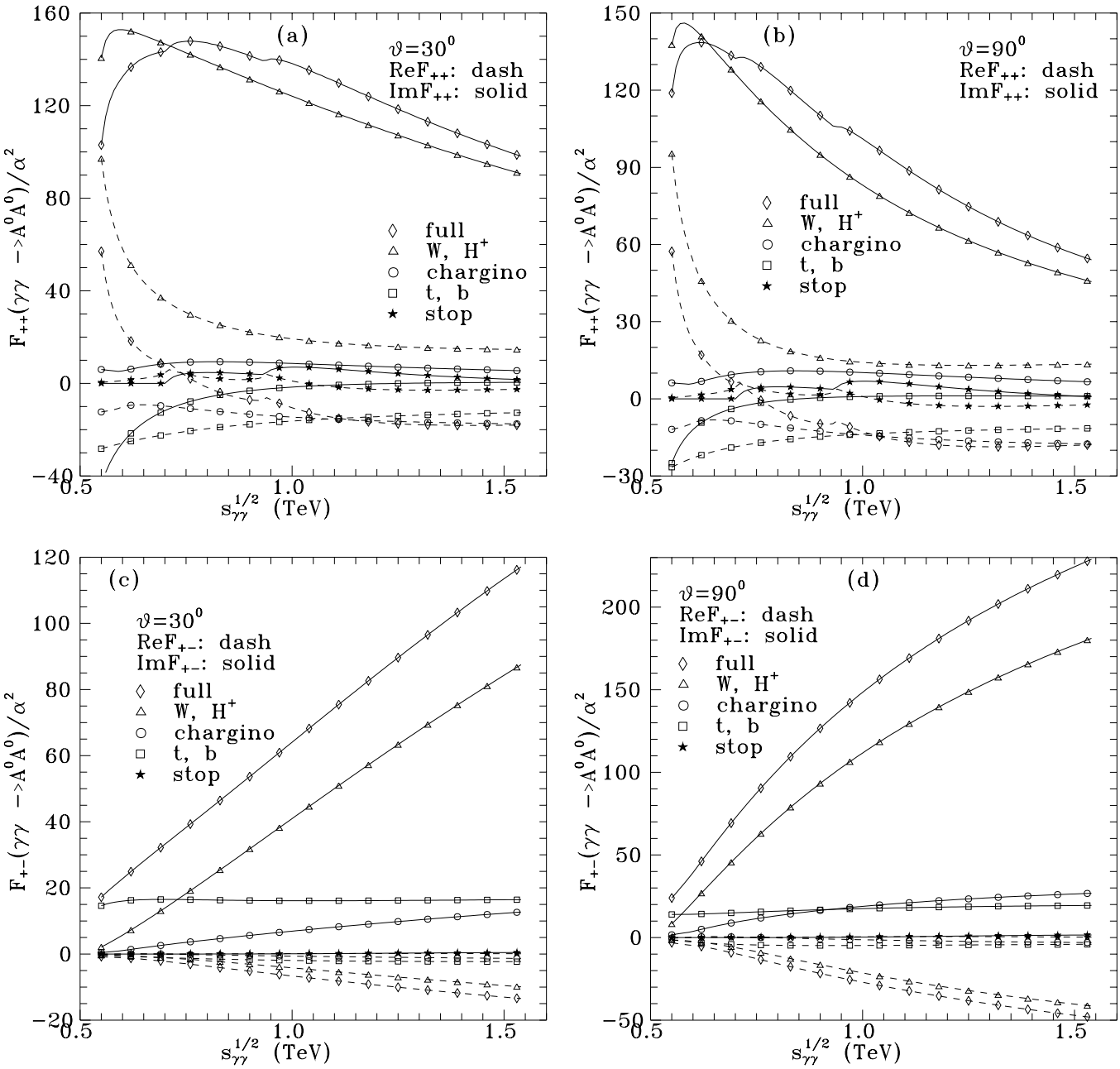

Fig. 6a–d. $\gamma\gamma \to A^0A^0$ helicity amplitudes as functions of the $\gamma\gamma$ center-of-mass energy $s_{\gamma gamma} \equiv \hat{s}$ for mSUGRA(2); see Table 1

ticularly sensitive to SUSY parameters like e.g. $\tan\beta$, but mainly depends on the A^0 mass. It should also be compared to the situation for single A^0 or H^0 production as studied in [27]. We also remark that a cross section at the 0.1–0.2 fb level may be observable if a luminosity of e.g. $\mathcal{L}_{\gamma\gamma} \sim 250\,\mathrm{fb}^{-1}$/year is realized in TESLA [2,3].

3 Conclusions

The Higgs sector, which is responsible for giving masses to almost all particles immediately after our Universe started, is definitely the most fascinating part of the present elementary particle theory. Motivated by this and assuming that the SUSY option is chosen by nature, we have studied here the process $\gamma\gamma \to A^0A^0$.

In the non-linear gauge used here, the types of contributing diagrams may be divided into two categories constructed on the basis of whether an s-channel neutral Higgs pole is involved or not. Each category may then be further divided into three classes, on the basis of whether their loops involve the $(W, H^{\pm})$ pair, charginos or sfermions. General formulae have been presented which

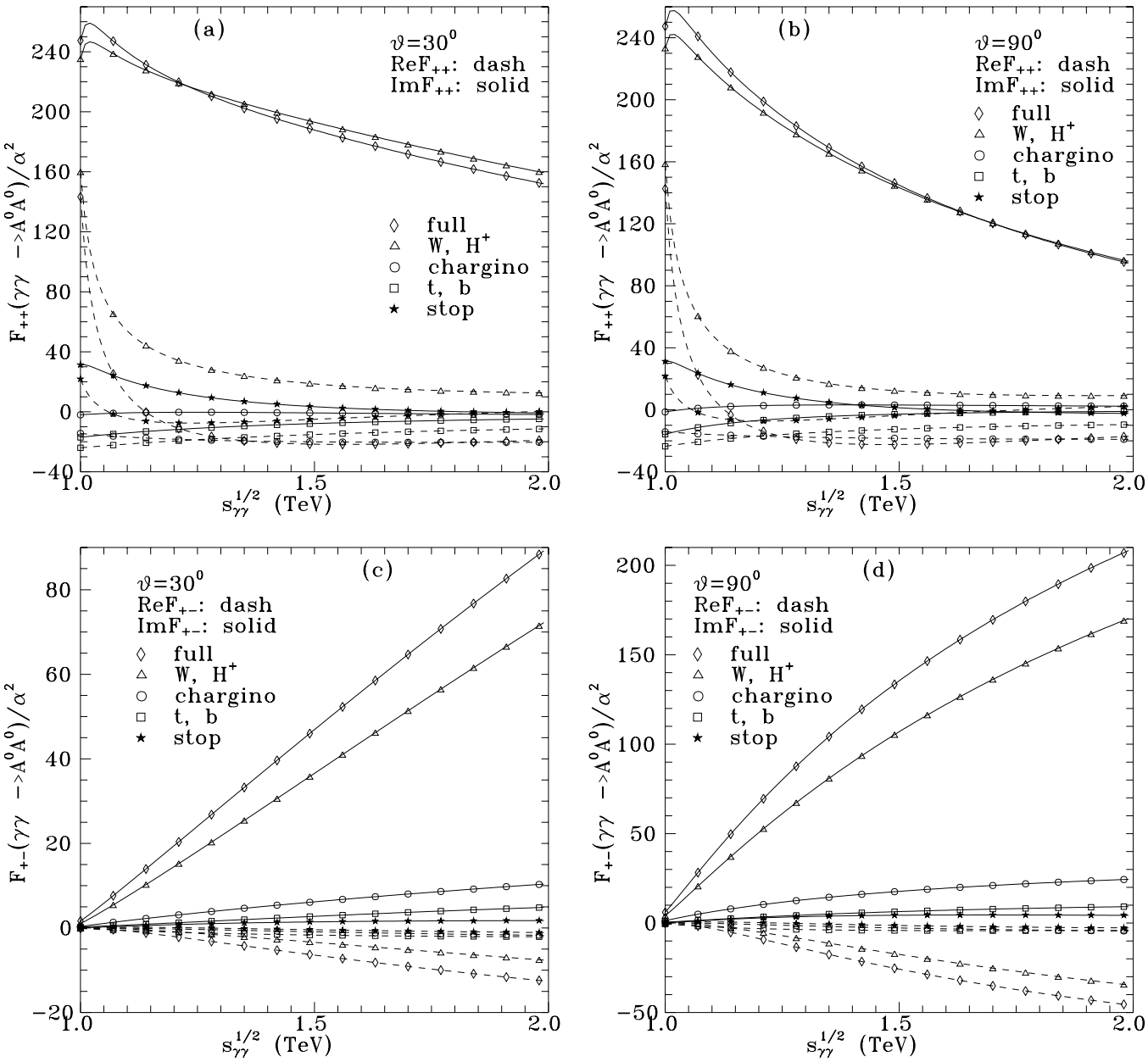

Fig. 7a–d. $\gamma\gamma \to A^0A^0$ helicity amplitudes as functions of the $\gamma\gamma$ center-of-mass energy $s_{\gamma\gamma} \equiv \hat{s}$ for mSUGRA(3); see Table 1

allow the description of the process in any SUSY model, minimal or non-minimal.

For the numerical applications we only considered three SUGRA examples presented in Table 1, leading to an A^0 heavier than $\sim$ 250 GeV. Excluding the forward and backward regions, the $\sigma(\gamma\gamma \to A^0A^0)$ cross section is found to be in the 0.1–0.2 fb region.

At sufficiently high energies, the two amplitudes F_{++} and F_{+-} are found to be to largely imaginary; an effect reminiscent (but not so predominant) to the one noticed in neutral gauge boson production [13,14]. On the contrary, nothing like this appears for the F_{++} amplitude in $\gamma\gamma \to h^0h^0$, in the standard model. It seems that the predominance of the imaginary part of a loop amplitude at high energies, is somehow associated with the predominance of a W-involving loop. The understanding of such properties may be useful for new physics searches; since e.g. for $\gamma\gamma \to \gamma\gamma$ they determine the way the interference between the "old" and possible forms of "new" physics may appear [28].

Thus, after the discovery of A^0 and the study of the single production process $\gamma\gamma \to A^0$ [11], the study of the double A^0 production through $\gamma\gamma \to A^0A^0$, should certainly be useful for verifying the Higgs identification.

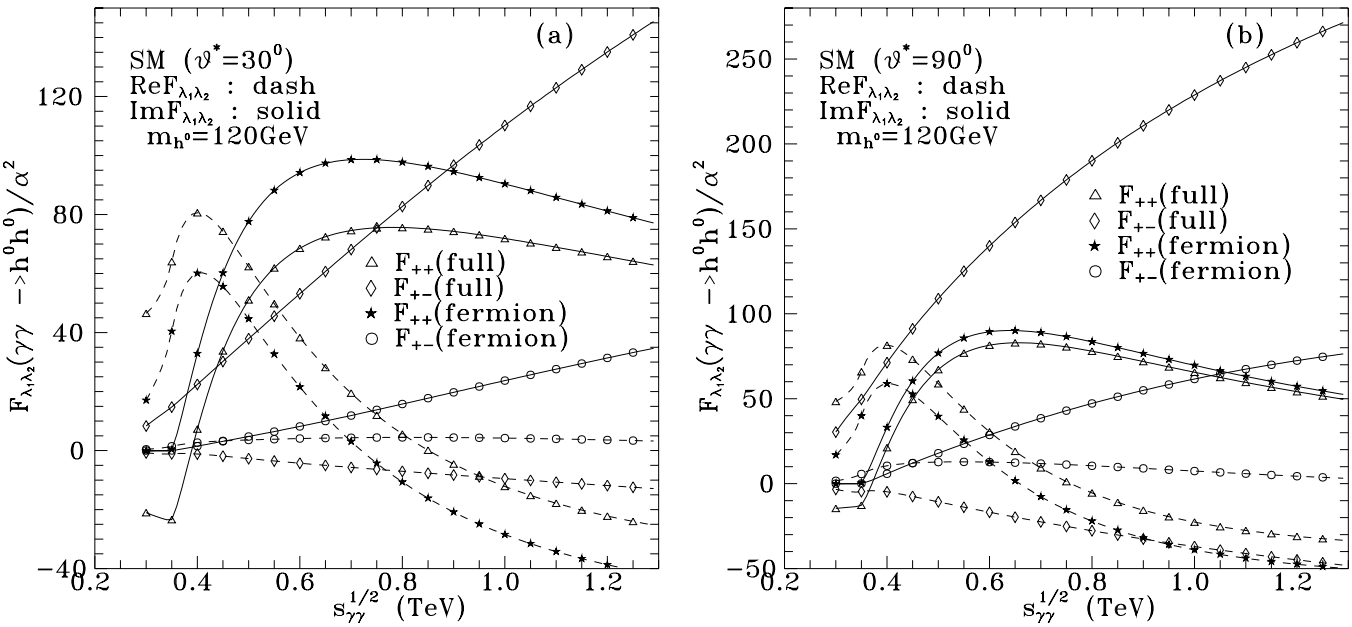

Fig. 8a,b. $\gamma\gamma \to h^0h^0$ helicity amplitudes as functions of the $\gamma\gamma$ center-of-mass energy $s_{\gamma\gamma} \equiv \hat{s}$ in SM. The SM fermion contribution is also separately given

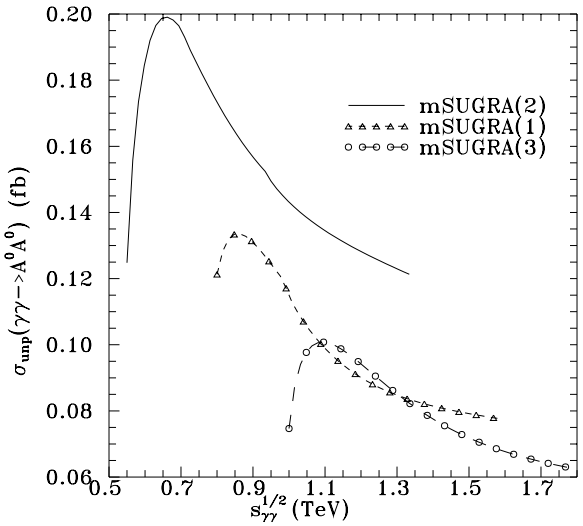

Fig. 9. Unpolarized total cross section for $\gamma\gamma \to A^0A^0$ in the region $30^0 < \vartheta^* < 150^0$ for the SUSY models SUGRA(1), SUGRA(2) and SUGRA(3); see Table 1

Appendix

A The MSSM vertices for $\gamma\gamma \to A^0A^0$

In order to reduce the number of diagrams contributing to $\gamma\gamma \to A^0A^0$, we use the nonlinear gauge defined by the gauge fixing term

$$\mathcal{L}_{GF} = -\frac{1}{\xi_W}F^+F^- - \frac{1}{2\xi_Z}(F_Z)^2 - \frac{1}{2\xi_\gamma}(F_\gamma)^2,$$
$$F^\pm = \partial^\mu W_\mu^\pm \pm \mathrm{i}\xi_W m_W G^\pm \pm \mathrm{i}g'B^\mu W_\mu^\pm,$$
$$F_Z = \partial^\mu Z_\mu + \xi_Z m_Z G^0,$$
$$F_\gamma = \partial^\mu A_\mu, \tag{A.1}$$

which is free from $\gamma W^\pm G^\mp$ and $ZW^\pm G^\mp$ vertices [24]. The implied ghost–photon and ghost–scalar field interactions then are

$$\begin{aligned}\mathcal{L}_{FP} = {} & \mathrm{i}eA_\mu(\partial^\mu\bar\eta^-\eta^+ - \partial^\mu\bar\eta^+\eta^- + \bar\eta^+\partial^\mu\eta^- - \bar\eta^-\partial^\mu\eta^+) \\ & + e^2A_\mu A^\mu(\bar\eta^+\eta^- + \bar\eta^-\eta^+) \\ & - \frac{1}{2}\xi_W g m_W(\bar\eta^+\eta^- + \bar\eta^-\eta^+) \\ & \times [\cos(\alpha-\beta)H^0 + \sin(\beta-\alpha)h^0].\end{aligned} \tag{A.2}$$

The complete list of diagrams contributing to the process $\gamma\gamma \to A^0A^0$ in the present gauge appears in Figs. 1–4. Below we give the interaction Lagrangian describing the vertices for these sets of diagrams.

The diagrams in Fig. 1 describe the $(H^\pm, W^\pm)$ loop contribution (together of course with the accompanying ghost and Goldstone ones). The relevant vertices involve, in addition to the gauge boson self-interactions present in SM, also the triple and quartic vertices [9]

$$\begin{aligned}\mathcal{L}_{VH} = {} & -\frac{g}{2}[(A^0\overleftrightarrow{\partial}^\mu H^-)W_\mu^+ + (A^0\overleftrightarrow{\partial}^\mu H^+)W_\mu^-] \\ & + \mathrm{i}\frac{gm_W}{2}(A^0H^-G^+ - A^0H^+G^-) \\ & + gm_W[\cos(\beta-\alpha)H^0 + \sin(\beta-\alpha)h^0]W_\mu^+W^{-\mu} \\ & - \mathrm{i}e(H^-\overleftrightarrow{\partial}^\mu H^+)A_\mu \\ & + \frac{gm_W}{2c_W^2}\cos 2\beta[\sin(\alpha+\beta)h^0 - \cos(\alpha+\beta)H^0]G^+G^- \\ & + \frac{gm_W}{4c_W^2}\cos 2\beta[\cos(\alpha+\beta)H^0 - \sin(\alpha+\beta)h^0]A^0A^0 \\ & + gm_W\left[\sin(\alpha-\beta) - \frac{\cos 2\beta}{2c_W^2}\sin(\alpha+\beta)\right]h^0H^+H^-\end{aligned}$$

$$
\begin{aligned}
&- gm_W\left[\cos(\alpha-\beta) - \frac{\cos 2\beta}{2c_{\rm W}^2}\cos(\alpha+\beta)\right] H^0H^+H^- \\
&+ \frac{g^2}{4}\left[W_\mu^+W^{-\mu} - \left(1-\frac{\cos^2 2\beta}{2c_{\rm W}^2}\right)G^+G^- \right. \\
&\left. - \frac{\cos^2 2\beta}{2c_{\rm W}^2}H^+H^-\right] A^0A^0 \\
&+ {\rm i}\frac{ge}{2}A^\mu A^0[W_\mu^+H^- - W_\mu^-H^+] \\
&+ e^2H^+H^-A_\mu A^\mu. \qquad \text{(A.3)}
\end{aligned}
$$

On the basis of this we define the h^0 couplings[5]

$$
\begin{aligned}
g_{h\bar\eta\eta} &\equiv -\frac{1}{2}\xi_W g m_W \sin(\beta-\alpha), \\
g_{hWW} &\equiv g m_W \sin(\beta-\alpha), \\
g_{hGG} &\equiv \frac{g m_W}{2c_{\rm W}^2}\cos 2\beta \sin(\alpha+\beta), \\
g_{hAA} &\equiv -\frac{g m_W}{2c_{\rm W}^2}\cos 2\beta \sin(\alpha+\beta), \\
g_{hH^+H^-} &= g m_W\left[\sin(\alpha-\beta) - \frac{\cos 2\beta}{2c_{\rm W}^2}\sin(\alpha+\beta)\right],
\end{aligned}
\qquad \text{(A.4)}
$$

and the H^0 couplings

$$
\begin{aligned}
g_{H^0\bar\eta\eta} &\equiv -\frac{1}{2}\xi_W g m_W \cos(\beta-\alpha), \\
g_{H^0WW} &\equiv g m_W \cos(\beta-\alpha), \\
g_{H^0GG} &\equiv -\frac{g m_W}{2c_{\rm W}^2}\cos 2\beta \cos(\alpha+\beta), \\
g_{H^0AA} &\equiv \frac{g m_W}{2c_{\rm W}^2}\cos 2\beta \cos(\alpha+\beta), \\
g_{H^0H^+H^-} &= -g m_W\left[\cos(\alpha-\beta) - \frac{\cos 2\beta}{2c_{\rm W}^2}\cos(\alpha+\beta)\right],
\end{aligned}
\qquad \text{(A.5)}
$$

which are used in Appendix B for expressing the (Higgs-W) loop contribution of the diagrams in Fig. 1, as well as the s-channel (h^0, H^0)-pole diagrams contained in Figs. 2–4.

The *chargino* loop contribution is described by the diagrams in Fig. 2. To define them we first list the chargino mass matrix term as[6]

$$
\begin{aligned}
\mathcal{L}_{M_\chi} = &-\left(\tilde W^{-\tau}, \tilde H_1^{-\tau}\right)_{\rm L}\cdot C\cdot\begin{pmatrix} M_2 & \sqrt{2}m_W\sin\beta \\ \sqrt{2}m_W\cos\beta & +\mu\end{pmatrix} \\
&\times\begin{pmatrix}\tilde W^+ \\ \tilde H_2^+\end{pmatrix}_{\rm L} + \text{h.c.} \qquad \text{(A.6)}
\end{aligned}
$$

Assuming that in MSSM there no new sources of CP-violation, apart from those already known in the Yukawa part of SM, we take the quantities (M_2, μ) as real, but of arbitrary sign. C is the usual charge conjugation matrix, and the τ index indicates transposition of the spinorial field. In terms of

$$
\tilde D \equiv \left[(M_2^2+\mu^2+2m_W^2)^2 - 4(M_2\mu - m_W^2\sin(2\beta))^2\right]^{1/2}, \qquad \text{(A.7)}
$$

the physical chargino masses are expressed as

$$
m_{\tilde\chi_1,\tilde\chi_2} = \frac{1}{\sqrt{2}}[M_2^2+\mu^2+2m_W^2 \mp \tilde D]^{1/2}. \qquad \text{(A.8)}
$$

The mixing angles $\phi_{\rm R}, \phi_{\rm L}$ in the $(\tilde W^+, \tilde H_2^+)_{\rm L}$ and $(\tilde W^-, \tilde H_1^-)_{\rm L}$ sectors, respectively, are defined so that they always lie in the second quarter

$$
\frac{\pi}{2} \le \phi_{\rm L} < \pi, \quad \frac{\pi}{2} \le \phi_{\rm R} < \pi. \qquad \text{(A.9)}
$$

They are written as

$$
\begin{aligned}
\cos\phi_{\rm L} &= -\frac{1}{\sqrt{2\tilde D}}[\tilde D - M_2^2 + \mu^2 + 2m_W^2\cos 2\beta]^{1/2}, \\
\cos\phi_{\rm R} &= -\frac{1}{\sqrt{2\tilde D}}[\tilde D - M_2^2 + \mu^2 - 2m_W^2\cos 2\beta]^{1/2}.
\end{aligned}
\qquad \text{(A.10)}
$$

We always describe the chargino field so that it absorbs a positive chargino particle; i.e. $\tilde\chi_j \equiv \tilde\chi_j^+$ $(j=1,2)$. Using this and the sign quantities

$$
\begin{aligned}
\tilde{\mathcal{B}}_{\rm L} &= {\rm Sign}(\mu\sin\beta + M_2\cos\beta), \\
\tilde{\mathcal{B}}_{\rm R} &= {\rm Sign}(\mu\cos\beta + M_2\sin\beta), \\
\tilde\Delta_1 &= {\rm Sign}(M_2[\tilde D - M_2^2 + \mu^2 - 2m_W^2] - 2m_W^2\mu\sin 2\beta), \\
\tilde\Delta_2 &= {\rm Sign}(\mu[\tilde D - M_2^2 + \mu^2 + 2m_W^2] + 2m_W^2 M_2\sin 2\beta), \\
\tilde{\mathcal{B}}_{\rm LR} &\equiv {\rm Sign}\left(M_2\mu + \frac{\mu^2+M_2^2}{2}\sin 2\beta\right) = \tilde{\mathcal{B}}_{\rm L}\tilde{\mathcal{B}}_{\rm R}, \\
\tilde\Delta_{12} &\equiv {\rm Sign}(M_2\mu - m_W^2\sin 2\beta) = \tilde\Delta_1\tilde\Delta_2,
\end{aligned}
\qquad \text{(A.11)}
$$

the neutral gauge boson–chargino couplings are written as

$$
\begin{aligned}
\mathcal{L} = &-eA^\mu\bar{\tilde\chi}_j\gamma_\mu\tilde\chi_j - \frac{e}{2s_Wc_W}Z^\mu\bar{\tilde\chi}_j\left(\gamma_\mu g_{vj} - \gamma_\mu\gamma_5 g_{aj}\right)\tilde\chi_j \\
&- \frac{e}{2s_Wc_W}Z^\mu\left[\bar{\tilde\chi}_1\left(\gamma_\mu g_{v12} - \gamma_\mu\gamma_5 g_{a12}\right)\tilde\chi_2 + \text{h.c.}\right],
\end{aligned}
\qquad \text{(A.12)}
$$

with

$$
\begin{aligned}
g_{v1} &= \frac{3}{2} - 2s_W^2 + \frac{1}{4}[\cos 2\phi_{\rm L} + \cos 2\phi_{\rm R}], \\
g_{a1} &= -\frac{1}{4}[\cos 2\phi_{\rm L} - \cos 2\phi_{\rm R}], \qquad \text{(A.13)} \\
g_{v2} &= \frac{3}{2} - 2s_W^2 - \frac{1}{4}[\cos 2\phi_{\rm L} + \cos 2\phi_{\rm R}], \\
g_{a2} &= \frac{1}{4}[\cos 2\phi_{\rm L} - \cos 2\phi_{\rm R}], \qquad \text{(A.14)} \\
g_{v12} &= -\frac{{\rm Sign}(M_2)}{4}[\tilde{\mathcal{B}}_{\rm R}\tilde\Delta_{12}\sin 2\phi_{\rm R} + \tilde{\mathcal{B}}_{\rm L}\sin 2\phi_{\rm L}], \\
g_{a12} &= -\frac{{\rm Sign}(M_2)}{4}[\tilde{\mathcal{B}}_{\rm R}\tilde\Delta_{12}\sin 2\phi_{\rm R} - \tilde{\mathcal{B}}_{\rm L}\sin 2\phi_{\rm L}],
\end{aligned}
\qquad \text{(A.15)}
$$

[5] For the definition of the scalar sector mixing angles we follow the standard notation of, e.g., [10]

[6] The gaugino fields are defined so that they satisfy $C\bar{\tilde W}^{+\tau} = \tilde W^-$. In such a case there is no i in front of $\tilde W^\pm$ in (A.6)

where the sign factors $(\tilde{\mathcal{B}}_{\rm L}, \tilde{\mathcal{B}}_{\rm R}, \tilde{\Delta}_{12})$ are given in[7] (A.11).

The corresponding chargino-neutral Higgs vertices are

$$\begin{aligned}\mathcal{L}_{A^0} &= {\rm i}A^0[g_{A1}\bar{\tilde{\chi}}_1\gamma_5\tilde{\chi}_1 + g_{A2}\bar{\tilde{\chi}}_2\gamma_5\tilde{\chi}_2 \\ &+ \bar{\tilde{\chi}}_1\left(g_{As12}+\gamma_5 g_{Ap12}\right)\tilde{\chi}_2 - \bar{\tilde{\chi}}_2\left(g_{As12}-\gamma_5 g_{Ap12}\right)\tilde{\chi}_1] \\ &+ (g_{h1}h^0 + g_{H^01}H^0)\bar{\tilde{\chi}}_1\tilde{\chi}_1 + (g_{h2}h^0 + g_{H^02}H^0)\bar{\tilde{\chi}}_2\tilde{\chi}_2,\end{aligned} \tag{A.16}$$

where

$$\begin{aligned}g_{h1} &= -\frac{g\tilde{\Delta}_1}{\sqrt{2}}[-\tilde{\mathcal{B}}_{\rm L}\sin\alpha\cos\phi_{\rm R}\sin\phi_{\rm L} \\ &+ \tilde{\mathcal{B}}_{\rm R}\cos\alpha\sin\phi_{\rm R}\cos\phi_{\rm L}], \\ g_{H^01} &= -\frac{g\tilde{\Delta}_1}{\sqrt{2}}[\tilde{\mathcal{B}}_{\rm L}\cos\alpha\cos\phi_{\rm R}\sin\phi_{\rm L} \\ &+ \tilde{\mathcal{B}}_{\rm R}\sin\alpha\sin\phi_{\rm R}\cos\phi_{\rm L}], \\ g_{h2} &= \frac{g\tilde{\Delta}_2}{\sqrt{2}}[-\tilde{\mathcal{B}}_{\rm R}\sin\alpha\sin\phi_{\rm R}\cos\phi_{\rm L} \\ &+ \tilde{\mathcal{B}}_{\rm L}\cos\alpha\sin\phi_{\rm L}\cos\phi_{\rm R}], \\ g_{H^02} &= \frac{g\tilde{\Delta}_2}{\sqrt{2}}[\tilde{\mathcal{B}}_{\rm R}\cos\alpha\sin\phi_{\rm R}\cos\phi_{\rm L} \\ &+ \tilde{\mathcal{B}}_{\rm L}\sin\alpha\cos\phi_{\rm R}\sin\phi_{\rm L}], \\ g_{A1} &= -\frac{g\tilde{\Delta}_1}{\sqrt{2}}[\tilde{\mathcal{B}}_{\rm L}\sin\beta\cos\phi_{\rm R}\sin\phi_{\rm L} \\ &+ \tilde{\mathcal{B}}_{\rm R}\cos\beta\sin\phi_{\rm R}\cos\phi_{\rm L}], \\ g_{A2} &= \frac{g\tilde{\Delta}_2}{\sqrt{2}}[\tilde{\mathcal{B}}_{\rm R}\sin\beta\sin\phi_{\rm R}\cos\phi_{\rm L} \\ &+ \tilde{\mathcal{B}}_{\rm L}\cos\beta\sin\phi_{\rm L}\cos\phi_{\rm R}], \\ g_{As12} &= \frac{g{\rm Sign}(M_2)}{2\sqrt{2}} \\ &\times [\tilde{\mathcal{B}}_{\rm LR}(\tilde{\Delta}_1\cos\beta - \tilde{\Delta}_2\sin\beta)\sin\phi_{\rm R}\sin\phi_{\rm L} \\ &- (\tilde{\Delta}_1\sin\beta - \tilde{\Delta}_2\cos\beta)\cos\phi_{\rm L}\cos\phi_{\rm R}], \\ g_{Ap12} &= \frac{g{\rm Sign}(M_2)}{2\sqrt{2}} \\ &\times [\tilde{\mathcal{B}}_{\rm LR}(\tilde{\Delta}_1\cos\beta + \tilde{\Delta}_2\sin\beta)\sin\phi_{\rm R}\sin\phi_{\rm L} \\ &- (\tilde{\Delta}_1\sin\beta + \tilde{\Delta}_2\cos\beta)\cos\phi_{\rm L}\cos\phi_{\rm R}].\end{aligned} \tag{A.17}$$

The appearance in (A.15) and (A.17) of the sign factors defined in (A.11) guarantees that the physical charginos always have positive masses, irrespective of the signs of the arbitrary real parameters M_2 and μ. These signs are of course intimately related to the definition of the chargino mixing angles employed in (A.9) and (A.10).

We next turn to the t- and b-quark loop contribution. The relevant diagrams for the t-quark case are shown in Fig. 3. The necessary vertices are determined by

$$\begin{aligned}\mathcal{L}_t &= -eA_\mu[Q_t\bar{t}\gamma^\mu t + Q_b\bar{b}\gamma^\mu b] \\ &+ {\rm i}\frac{g}{2m_W}A^0[m_t\cot\beta\bar{t}\gamma_5 t + m_b\tan\beta\bar{b}\gamma_5 b] \\ &- \frac{gm_t}{2m_W\sin\beta}[h^0\cos\alpha + H^0\sin\alpha]\bar{t}t \\ &- \frac{gm_b}{2m_W\cos\beta}[H^0\cos\alpha - h^0\sin\alpha]\bar{b}b,\end{aligned} \tag{A.18}$$

where Q_t, Q_b are the t- and b-quark charges. The implied t-quark couplings are

$$\begin{aligned}g_{h^0tt} &= -\frac{gm_t}{2m_W\sin\beta}\cos\alpha, \\ g_{H^0tt} &= -\frac{gm_t}{2m_W\sin\beta}\sin\alpha, \\ g_{Att} &= \frac{gm_t}{2m_W}\cot\beta,\end{aligned} \tag{A.19}$$

and correspondingly for the b couplings.

Finally, for the *stop* loop contribution, the relevant interaction Lagrangian is

$$\begin{aligned}\mathcal{L}_{\tilde{t}} &= -{\rm i}eQ_tA_\mu\left[(\tilde{t}_1^*\overset{\leftrightarrow\mu}{\partial}\tilde{t}_1) + (\tilde{t}_2^*\overset{\leftrightarrow\mu}{\partial}\tilde{t}_2)\right] \\ &+ e^2Q_t^2A_\mu A^\mu(\tilde{t}_1^*\tilde{t}_1 + \tilde{t}_2^*\tilde{t}_2) \\ &+ {\rm i}\frac{gm_t}{2m_W}(A_t\cot\beta + \mu)A^0[\tilde{t}_{\rm L}^*\tilde{t}_{\rm R} - \tilde{t}_{\rm R}^*\tilde{t}_{\rm L}] \\ &- \Bigg[\frac{gm_t^2\cos\alpha}{m_W\sin\beta} \\ &- g_Zm_Z\sin(\alpha+\beta)\left(T_t^{(3)} - Q_ts_{\rm W}^2\right)\Bigg]h^0\tilde{t}_{\rm L}^*\tilde{t}_{\rm L} \\ &- \left[\frac{gm_t^2\cos\alpha}{m_W\sin\beta} - Q_tg_Zm_Z\sin(\alpha+\beta)s_{\rm W}^2)\right]h^0\tilde{t}_{\rm R}^*\tilde{t}_{\rm R} \\ &- \frac{gm_t}{2m_W\sin\beta}(\mu\sin\alpha + A_t\cos\alpha)h^0(\tilde{t}_{\rm R}^*\tilde{t}_{\rm L} + \tilde{t}_{\rm L}^*\tilde{t}_{\rm R}) \\ &- \Bigg[\frac{gm_t^2\sin\alpha}{m_W\sin\beta} \\ &+ g_Zm_Z\cos(\alpha+\beta)\left(T_t^{(3)} - Q_ts_{\rm W}^2\right)\Bigg]H^0\tilde{t}_{\rm L}^*\tilde{t}_{\rm L} \\ &- \left[\frac{gm_t^2\sin\alpha}{m_W\sin\beta} + Q_tg_Zm_Z\cos(\alpha+\beta)s_{\rm W}^2)\right]H^0\tilde{t}_{\rm R}^*\tilde{t}_{\rm R} \\ &+ \frac{gm_t}{2m_W\sin\beta}(\mu\cos\alpha - A_t\sin\alpha)H^0(\tilde{t}_{\rm R}^*\tilde{t}_{\rm L} + \tilde{t}_{\rm L}^*\tilde{t}_{\rm R}) \\ &- \Bigg[\frac{g^2m_t^2}{4m_W^2}\cot^2\beta \\ &- \frac{1}{4}g_Z^2(T_t^{(3)} - s_{\rm W}^2Q_t)\cos2\beta\Bigg]A^0A^0\tilde{t}_{\rm L}^*\tilde{t}_{\rm L} \\ &- \left[\frac{g^2m_t^2}{4m_W^2}\cot^2\beta - \frac{1}{4}g_Z^2s_{\rm W}^2Q_t\cos2\beta\right]A^0A^0\tilde{t}_{\rm R}^*\tilde{t}_{\rm R},\end{aligned} \tag{A.20}$$

where, as usual, $g_Z = g/c_{\rm W}$. The various neutral Higgs–$\tilde{t}_{\rm L,R}$ couplings are determined from the coefficients of the various terms in (A.20). For two examples, we note[8]

$$g_{A\tilde{t}_{\rm L}\tilde{t}_{\rm R}} = \frac{gm_t}{2m_W}(A_t\cot\beta + \mu),$$

[7] These expressions are equivalent to those given, e.g., in [29], where a more common definition of the $\phi_{\rm L,R}$-angles is employed

[8] As usual, in the definition of the $A^0A^0\tilde{t}_{\rm L}^*\tilde{t}_{\rm L}$ and $A^0A^0\tilde{t}_{\rm R}^*\tilde{t}_{\rm R}$ couplings from the last two terms in (A.20), the relevant coefficient is multiplied by 2, due to the identity of the two A^0 fields

$$g_{AA\tilde{t}_R\tilde{t}_R} = -2\left[\frac{g^2 m_t^2}{4m_W^2}\cot^2\beta - \frac{1}{4}g_Z^2 s_W^2 Q_t \cos 2\beta\right].$$

For determining the corresponding couplings to the physical $\tilde{t}_{1,2}$ we write

$$\begin{pmatrix}\tilde{t}_L\\ \tilde{t}_R\end{pmatrix} = \begin{pmatrix}\cos\theta_t & -\sin\theta_t \mathrm{Sign}(A_t-\mu\cot\beta)\\ \sin\theta_t \mathrm{Sign}(A_t-\mu\cot\beta) & \cos\theta_t\end{pmatrix} \times \begin{pmatrix}\tilde{t}_1\\ \tilde{t}_2\end{pmatrix}, \tag{A.21}$$

where θ_t is fully determined by[9]

$$\sin(2\theta_t) = \frac{2m_t|A_t - \mu\cot\beta|}{m_{\tilde{t}_1}^2 - m_{\tilde{t}_2}^2},$$
$$\cos(2\theta_t) = \frac{m_{\tilde{t}_L}^2 - m_{\tilde{t}_R}^2}{m_{\tilde{t}_1}^2 - m_{\tilde{t}_2}^2}, \tag{A.22}$$

while A_t is also real. We observe from (A.22) that

$$\frac{\pi}{2} < \theta_t < \pi,$$

since $m_{\tilde{t}_1} < m_{\tilde{t}_2}$, by definition. We have checked that this stop-mixing-formalism is equivalent to the usual one found, e.g., in [9,10,30,14].

B The MSSM contributions to $\gamma\gamma \to A^0A^0$

The invariant helicity amplitudes for the process

$$\gamma(p_1,\lambda_1)\gamma(p_2,\lambda_2) \to A^0(p_3)A^0(p_4) \tag{B.1}$$

are denoted as[10] $F_{\lambda_1\lambda_2}(\hat{s},\hat{t},\hat{u})$, where the particle momenta and helicities of the incoming photons are indicated in parentheses. Assuming no new (beyond SM) source of CP-violation, these invariant helicity amplitudes satisfy

$$F_{\lambda_1,\lambda_2}(\hat{s},\hat{t},\hat{u}) = F_{-\lambda_1,-\lambda_2}(\hat{s},\hat{t},\hat{u}), \tag{B.2}$$

which implies that there are only two independent helicity amplitudes; namely F_{++} and F_{+-}. As in [14] we make the definitions

$$\hat{s} = (p_1+p_2)^2 = \frac{4m_A^2}{1-\beta_A^2},$$
$$\hat{t} = (p_1-p_3)^2, \quad \hat{u} = (p_1-p_4)^2, \tag{B.3}$$
$$\hat{s}_4 = \hat{s} - 4m_A^2, \quad \hat{s}_2 = \hat{s} - 2m_A^2,$$
$$\hat{t}_1 = \hat{t} - m_A^2, \quad \hat{u}_1 = \hat{u} - m_A^2, \tag{B.4}$$
$$\hat{t} = m_A^2 - \frac{\hat{s}}{2}(1-\beta_A\cos\vartheta^*),$$
$$\hat{u} = m_A^2 - \frac{\hat{s}}{2}(1+\beta_A\cos\vartheta^*), \tag{B.5}$$
$$Y = \hat{t}\hat{u} - m_A^4 = \frac{\hat{s}^2\beta_A^2}{4}\sin^2\vartheta^*, \tag{B.6}$$

where β_A is the A^0-velocity in the A^0A^0-c.m. frame, and ϑ^* the c.m. scattering angle. Moreover, the combinations

$$m_{ab}^2 = m_A^2 + m_a^2 - m_b^2, \quad \hat{s}_{ab} = \hat{s} - m_{ab}^2 \tag{B.7}$$

often appear below for the charged particle pairs $(a,b) = (H^\pm, W^\mp)$, $(W^\mp, H^\pm)$ and $(\tilde{\chi}_1, \tilde{\chi}_2)$.

All 1-loop results are expressed in terms of the C_0 and D_0 Passarino–Veltman functions [15], for which we follow the notation of [31]. Similarly to [14], we also introduce the short hand writing[11]

$$C_0^{abc}(\hat{s}) \equiv C_0(k_1,k_2) = C_0(0,0,\hat{s};m_a,m_b,m_c), \tag{B.8}$$
$$C_A^{abc}(\hat{t}) \equiv C_0(k_3,k_1) = C_0(m_A^2,0,\hat{t};m_a,m_b,m_c), \tag{B.9}$$
$$C_{AA}^{abc}(\hat{s}) \equiv C_0(k_3,k_4) = C_0(m_A^2,m_A^2,\hat{s};m_a,m_b,m_c), \tag{B.10}$$
$$D_{AA}^{abcd}(\hat{s},\hat{t}) \equiv D_0(k_4,k_3,k_1) = D_0(m_A^2,m_A^2,0,0,\hat{s},\hat{t};m_a,m_b,m_c,m_d), \tag{B.11}$$
$$D_{AA}^{abcd}(\hat{s},\hat{u}) \equiv D_0(k_3,k_4,k_1) = D_0(m_A^2,m_A^2,0,0,\hat{s},\hat{u};m_a,m_b,m_c,m_d), \tag{B.12}$$
$$D_{AA}^{abcd}(\hat{t},\hat{u}) \equiv D_0(k_3,k_1,k_4) = D_0(m_A^2,0,m_A^2,0,\hat{t},\hat{u};m_a,m_b,m_c,m_d), \tag{B.13}$$
$$D_{AA}^{abcd}(\hat{u},\hat{t}) \equiv D_0(k_4,k_1,k_3) = D_0(m_A^2,0,m_A^2,0,\hat{u},\hat{t};m_a,m_b,m_c,m_d), \tag{B.14}$$

in which we have also emphasized the fact that the masses running along the various sides of the loop may be different.

The fact that the masses along the loops in Figs. 1, 2 and 4 may be different considerably complicates the formulae. Nevertheless, expressions analogous to those encountered for the SM contributions to $\gamma\gamma \to ZZ$ [14] may be defined, which allows one to write the amplitudes in a compact way. We thus define

$$\tilde{F}^{ab}(\hat{s},\hat{t},\hat{u}) = D_{AA}^{abba}(\hat{t},\hat{u}) + D_{AA}^{abaa}(\hat{s},\hat{t}) + D_{AA}^{abaa}(\hat{s},\hat{u}), \tag{B.15}$$
$$E_1^{ab}(\hat{s},\hat{t}) = \hat{t}_1\left[C_A^{abb}(\hat{t}) + C_A^{baa}(\hat{t})\right] - \hat{s}\hat{t}D_{AA}^{abaa}(\hat{s},\hat{t}), \tag{B.16}$$
$$E_2^{ab}(\hat{t},\hat{u}) = \hat{t}_1\left[C_A^{abb}(\hat{t}) + C_A^{baa}(\hat{t})\right] + \hat{u}_1\left[C_A^{abb}(\hat{u}) + C_A^{baa}(\hat{u})\right] - YD_{AA}^{abba}(\hat{t},\hat{u}), \tag{B.17}$$

[9] The quantities $m_{\tilde{t}_L}^2$, $m_{\tilde{t}_R}^2$ in (A.22) are the usual soft SUSY breaking parameters in which the small D contributions have also been included

[10] Their sign is related to the sign of the S-matrix through $S_{\lambda_1\lambda_2} = 1 + \mathrm{i}(2\pi)^4\delta(p_f - p_i)F_{\lambda_1\lambda_2}$

[11] In the middle terms of (B.8)–(B.13) $k_1 = p_1$, $k_2 = p_2$ denote the momenta of the photons, while $k_3 = -p_3$, $k_4 = -p_4$ are those of the A^0, always taken as incoming; compare (B.1)

which are closely related to the definitions in (A.22)–(A.24) in [14]. We also note that

$$\begin{aligned} &D_{AA}^{abba}(\hat{t},\hat{u}) = D_{AA}^{abba}(\hat{u},\hat{t}) = D_{AA}^{baab}(\hat{t},\hat{u}) = D_{AA}^{baab}(\hat{u},\hat{t}),\\ &\tilde{F}^{ab}(\hat{s},\hat{t},\hat{u}) = \tilde{F}^{ab}(\hat{s},\hat{u},\hat{t}),\\ &E_2^{ab}(\hat{t},\hat{u}) = E_2^{ab}(\hat{u},\hat{t}) = E_2^{ba}(\hat{t},\hat{u}). \end{aligned} \tag{B.18}$$

The $(W^{\pm}, H^{\pm})$-loop diagrams

There two kinds of contributions to the invariant amplitudes $F_{\lambda_1\lambda_2}(\gamma\gamma \to A^0A^0)$ from the diagrams of Fig. 1. The first arises from the two diagrams in the first row of Fig. 1 and contains $\hat{s}$-pole contributions generated by exchanging the CP-even neutral Higgs particles h^0 and H^0. For the $\hat{s}$-channel h^0 case, this is given by

$$\begin{aligned} &F_{++}^{WH^{\pm}(h^0\text{-pole})}\\ &= \frac{e^2 g_{hAA}}{8\pi^2(\hat{s}-m_h^2)}\\ &\times\{g_{hH^+H^-}[1+2m_{H^{\pm}}^2 C_0^{H^+H^+H^+}(\hat{s})]\\ &+g_{hGG}-2g_{h\eta\eta}\\ &-4g_{hWW}+2\left[(g_{hGG}-2g_{h\eta\eta}-4g_{hWW})m_W^2\right.\\ &\left.+2g_{hWW}\hat{s}\right]C_0^{WWW}(\hat{s})\}, \end{aligned} \tag{B.19}$$

while for the H^0 case we get

$$F_{++}^{WH^{\pm}(H^0\text{-pole})} = F_{++}^{WH^{\pm}(h^0\text{-pole})}(h^0 \to H^0), \tag{B.20}$$

where the needed h^0 and H^0 couplings are given in (A.4) and (A.5). For such contributions we obviously also have

$$F_{+-}^{WH^{\pm}(H^0\text{-pole})} = F_{+-}^{WH^{\pm}(h^0\text{-pole})} = 0. \tag{B.21}$$

The second comes from the 3rd to last diagrams in Fig. 1, and it is written as

$$\begin{aligned} F_{++}^{WH^{\pm}} &= \frac{e^2g^2}{16\pi^2}\left\{4+\left[6-\frac{\cos^2(2\beta)}{c_{\rm W}^2}\right]m_W^2 C_0^{WWW}(\hat{s})\right.\\ &+\left[2+\frac{\cos^2(2\beta)}{c_{\rm W}^2}\right]m_{H^{\pm}}^2 C_0^{H^{\pm}H^{\pm}H^{\pm}}(\hat{s})\\ &+2\frac{m_{HW}^2}{\hat{s}}E_2^{H^{\pm}W}(\hat{t},\hat{u})\\ &+2m_{H^{\pm}}^2\hat{s}_{HW}\tilde{F}^{H^{\pm}W}(\hat{s},\hat{t},\hat{u})\\ &\left.+2(\hat{s}m_{H^{\pm}}^2-m_{HW}^2m_W^2)\tilde{F}^{WH^{\pm}}(\hat{s},\hat{t},\hat{u})\right\}, \end{aligned} \tag{B.22}$$

$$\begin{aligned} F_{+-}^{WH^{\pm}} &= \frac{e^2g^2}{16\pi^2 Y}\{\hat{s}\left[2(m_{HW}^2m_{WH}^2-Y)\right.\\ &+\left.\hat{s}(m_H^2-m_W^2)+\hat{t}\hat{t}_1+\hat{u}\hat{u}_1\right]C_0^{WWW}(\hat{s})\\ &+\hat{s}\hat{s}_{HW}(\hat{s}_{HW}-m_{HW}^2)C_0^{H^{\pm}H^{\pm}H^{\pm}}(\hat{s})\\ &+\hat{s}_{HW}(\hat{t}^2+\hat{u}^2-2m_A^4)\\ &\times\left[C_{AA}^{H^{\pm}WH^{\pm}}(\hat{s})+C_{AA}^{WH^{\pm}W}(\hat{s})\right]\\ &+2\left[\hat{s}\hat{s}_{HW}(m_{H^{\pm}}^2-m_W^2)^2\right.\\ &+Y\left[2\hat{s}m_W^2+Y-m_{HW}^2(m_W^2+m_{H^{\pm}}^2)\right]\\ &\times\tilde{F}^{WH^{\pm}}(\hat{s},\hat{t},\hat{u})\\ &+\{\hat{s}_{HW}\left[\hat{s}(m_{H^{\pm}}^2-m_W^2)^2\right.\\ &+\left.\hat{s}\hat{t}(\hat{t}-2m_W^2)-2m_{H^{\pm}}^2\hat{t}_1^2\right]\\ &\times\left[D_{AA}^{H^{\pm}WH^{\pm}H^{\pm}}(\hat{s},\hat{t})-D_{AA}^{WH^{\pm}WW}(\hat{s},\hat{t})\right]\\ &+2(m_A^4+\hat{t}^2-\hat{t}m_{WH}^2)E_1^{WH^{\pm}}(\hat{s},\hat{t})+(\hat{t}\leftrightarrow\hat{u})\}\}, \end{aligned} \tag{B.23}$$

where all needed quantities have been defined in (B.3)–(B.17).

The chargino loop diagrams

The relevant diagrams are presented in Fig. 2. The first diagram in Fig. 2 contains an $\hat{s}$-channel pole due to (h^0, H^0) exchanges, and is characterized by a single chargino $\tilde{\chi}_i$ running along the loop. It gives

$$\begin{aligned} F_{++}^{\tilde{\chi}_i(\text{pole})} &= -\frac{e^2m_{\tilde{\chi}_i}}{4\pi^2}\left(\frac{g_{hi}g_{hAA}}{\hat{s}-m_h^2}+\frac{g_{Hi}g_{H^0AA}}{\hat{s}-m_H^2}\right)\\ &\times\left[2+(4m_{\tilde{\chi}_i}^2-\hat{s})C_0^{\tilde{\chi}_i\tilde{\chi}_i\tilde{\chi}_i}(\hat{s})\right], \end{aligned} \tag{B.24}$$

$$F_{+-}^{\tilde{\chi}_i(\text{pole})} = 0. \tag{B.25}$$

The other diagrams in Fig. 2 involve contributions containing either a single chargino running along the loop, or mixed contributions where both charginos run. The single chargino contribution is

$$\begin{aligned} F_{++}^{\tilde{\chi}_i} &= -\frac{e^2g_{Ai}^2}{4\pi^2}\left\{2+4m_{\tilde{\chi}_i}^2C_0^{\tilde{\chi}_i\tilde{\chi}_i\tilde{\chi}_i}(\hat{s})\right.\\ &-\left.m_{\tilde{\chi}_i}^2(\hat{t}+\hat{u})\tilde{F}^{\tilde{\chi}_i\tilde{\chi}_i}(\hat{s},\hat{t},\hat{u})+\frac{m_A^2}{\hat{s}}E_2^{\tilde{\chi}_i\tilde{\chi}_i}(\hat{t},\hat{u})\right\}, \end{aligned} \tag{B.26}$$

$$\begin{aligned} F_{+-}^{\tilde{\chi}_i} &= -\frac{e^2g_{Ai}^2}{8\pi^2Y}\{\hat{s}(\hat{s}_2^2-2Y)C_0^{\tilde{\chi}_i\tilde{\chi}_i\tilde{\chi}_i}(\hat{s})\\ &+\hat{s}_2(\hat{t}^2+\hat{u}^2-2m_A^4)C_{AA}^{\tilde{\chi}_i\tilde{\chi}_i\tilde{\chi}_i}(\hat{s})\\ &+2m_{\tilde{\chi}_i}^2\hat{s}_2Y\tilde{F}^{\tilde{\chi}_i\tilde{\chi}_i}(\hat{s},\hat{t},\hat{u})+(\hat{t}^2+m_A^4)E_1^{\tilde{\chi}_i\tilde{\chi}_i}(\hat{s},\hat{t})\\ &+(\hat{u}^2+m_A^4)E_1^{\tilde{\chi}_i\tilde{\chi}_i}(\hat{s},\hat{u})\}. \end{aligned} \tag{B.27}$$

Of course, in calculating the total "single" chargino contribution, the results in (B.24)–(B.27) should be summed for both the $\tilde{\chi}_1$ and $\tilde{\chi}_2$ charginos. The necessary couplings are given in (A.17).

The considerably more complicated mixed chargino contribution, arising from the 3rd and 4th diagram in Fig. 2, is

$$\begin{aligned} F_{++}^{\tilde{\chi}_1\tilde{\chi}_2} &= -\frac{e^2}{4\pi^2}(g_{As12}^2+g_{Ap12}^2)\left\{2+4m_{\tilde{\chi}_1}^2C_0^{\tilde{\chi}_1\tilde{\chi}_1\tilde{\chi}_1}(\hat{s})\right.\\ &+\frac{1}{2\hat{s}}(\hat{s}-X)E_2^{\tilde{\chi}_1\tilde{\chi}_2}(\hat{t},\hat{u})-m_{\tilde{\chi}_1}\\ &\times\left[\hat{s}\left(m_{\tilde{\chi}_1}+\frac{(g_{As12}^2-g_{Ap12}^2)}{(g_{As12}^2+g_{Ap12}^2)}m_{\tilde{\chi}_2}\right)-m_{\tilde{\chi}_1}X\right] \end{aligned}$$

$$\times\ \tilde{F}^{\tilde{\chi}_1\tilde{\chi}_2}(\hat{s},\hat{t},\hat{u}) + (\tilde{\chi}_1 \leftrightarrow \tilde{\chi}_2)\Big\}, \tag{B.28}$$

$$\begin{aligned}
F_{+-}^{\tilde{\chi}_1\tilde{\chi}_2} &= -\frac{e^2(g_{As12}^2+g_{Ap12}^2)}{8\pi^2 Y}\\
&\times \{\hat{s}\left[X(\hat{s}_{\tilde{\chi}_1\tilde{\chi}_2}-m_{\tilde{\chi}_1\tilde{\chi}_2})-2Y\right]C_0^{\tilde{\chi}_1\tilde{\chi}_1\tilde{\chi}_1}(\hat{s})\\
&+ X\left[(m_{\tilde{\chi}_1}^2+m_{\tilde{\chi}_2}^2)Y+\hat{s}(m_{\tilde{\chi}_1}^2-m_{\tilde{\chi}_2}^2)^2\right]\\
&\times \tilde{F}^{\tilde{\chi}_1\tilde{\chi}_2}(\hat{s},\hat{t},\hat{u})\\
&+ X(\hat{t}^2+\hat{u}^2-2m_A^4)C_{AA}^{\tilde{\chi}_1\tilde{\chi}_2\tilde{\chi}_1}(\hat{s})\\
&- (\hat{t}X+Y)E_1^{\tilde{\chi}_1\tilde{\chi}_2}(\hat{s},\hat{t})\\
&- (\hat{u}X+Y)E_1^{\tilde{\chi}_1\tilde{\chi}_2}(\hat{s},\hat{u})\\
&- (m_{\tilde{\chi}_1}^2-m_{\tilde{\chi}_2}^2)\left[2\hat{t}_1^2X+Y(X-\hat{s})\right]\\
&\times D_{AA}^{\tilde{\chi}_1\tilde{\chi}_2\tilde{\chi}_1\tilde{\chi}_1}(\hat{s},\hat{t}) - (m_{\tilde{\chi}_1}^2-m_{\tilde{\chi}_2}^2)\\
&\times \left[2\hat{u}_1^2X+Y(X-\hat{s})\right]D_{AA}^{\tilde{\chi}_1\tilde{\chi}_2\tilde{\chi}_1\tilde{\chi}_1}(\hat{s},\hat{u})\\
&+ (\tilde{\chi}_1 \leftrightarrow \tilde{\chi}_2)\},
\end{aligned} \tag{B.29}$$

where

$$X = \hat{s}_2 + 2m_{\tilde{\chi}_1}^2 + 2m_{\tilde{\chi}_2}^2 + 4m_{\tilde{\chi}_1}m_{\tilde{\chi}_2}\frac{(g_{As12}^2-g_{Ap12}^2)}{(g_{As12}^2+g_{Ap12}^2)}, \tag{B.30}$$

and the necessary couplings are given in (A.17).

The t- and b-quark loop diagrams

The top-loop contribution arises from the diagrams in Fig. 3. The first of them contains the (h^0, H^0)-pole contribution

$$\begin{aligned}
F_{++}^{t(\mathrm{pole})} &= -\frac{3e^2Q_t^2m_t}{4\pi^2}\left(\frac{g_{htt}g_{hAA}}{\hat{s}-m_h^2}+\frac{g_{H^0tt}g_{H^0AA}}{\hat{s}-m_H^2}\right)\\
&\times \left[2+(4m_t^2-\hat{s})C_0^{ttt}(\hat{s})\right],
\end{aligned} \tag{B.31}$$

$$F_{+-}^{t(\mathrm{pole})} = 0, \tag{B.32}$$

while the second gives

$$\begin{aligned}
F_{++}^{t} &= -\frac{3e^2Q_t^2g_{Att}^2}{4\pi^2}\left[2+4m_t^2C_0^{ttt}(\hat{s})\right.\\
&\left.- m_t^2(\hat{t}+\hat{u})\tilde{F}^{tt}(\hat{s},\hat{t},\hat{u}) + \frac{m_A^2}{\hat{s}}E_2^{tt}(\hat{t},\hat{u})\right],
\end{aligned} \tag{B.33}$$

$$\begin{aligned}
F_{+-}^{t} &= -\frac{3e^2Q_t^2g_{Att}^2}{8\pi^2 Y}\{\hat{s}(\hat{s}_2^2-2Y)C_0^{ttt}(\hat{s})\\
&+ \hat{s}_2(\hat{t}^2+\hat{u}^2-2m_A^4)C_{AA}^{ttt}(\hat{s}) + 2m_t^2\hat{s}_2Y\tilde{F}^{tt}(\hat{s},\hat{t},\hat{u})\\
&+ (\hat{t}^2+m_A^4)E_1^{tt}(\hat{s},\hat{t}) + (\hat{u}^2+m_A^4)E_1^{tt}(\hat{s},\hat{u})\}.
\end{aligned} \tag{B.34}$$

All needed couplings are given in (A.4), (A.5) and (A.19). In (B.31)–(B.34) a factor three for color has already been introduced. The corresponding b-quark contribution is analogously obtained through (A.18) and the use of Q_b instead of Q_t.

$\tilde{t}$-loop diagrams

These diagrams are shown in Fig. 4 and will be relevant in the case that one or two stop sqarks turn out to be not too heavy. The first two of these diagrams describe the (h^0, H^0) $\hat{s}$-channel pole contributions and have just one kind of $\tilde{t}_i$ running along the loop. For each such $\tilde{t}_i$, the pole contribution is

$$\begin{aligned}
F_{++}^{\tilde{t}_i(\mathrm{pole})} &= \frac{3e^2Q_t^2}{8\pi^2}\left(\frac{g_{hAA}g_{h\tilde{t}_i\tilde{t}_i}}{\hat{s}-m_h^2}+\frac{g_{HAA}g_{H\tilde{t}_i\tilde{t}_i}}{\hat{s}-m_H^2}\right)\\
&\times \left[1+2m_{\tilde{t}_i}^2C_0^{\tilde{t}_i\tilde{t}_i\tilde{t}_i}(\hat{s})\right],
\end{aligned} \tag{B.35}$$

$$F_{+-}^{\tilde{t}_i(\mathrm{pole})} = 0. \tag{B.36}$$

In addition, we have the loop contribution from the no-pole last five diagrams of Fig. 4

$$\begin{aligned}
F_{++}^{\tilde{t}_1\tilde{t}_2} &= -\frac{3e^2Q_t^2}{8\pi^2}\left\{g_{AA\tilde{t}_1\tilde{t}_1}\left[1+2m_{\tilde{t}_1}^2C_0^{\tilde{t}_1\tilde{t}_1\tilde{t}_1}(\hat{s})\right]\right.\\
&+ \frac{g_{A\tilde{t}_1\tilde{t}_2}^2}{\hat{s}}E_2^{\tilde{t}_1\tilde{t}_2}(\hat{t},\hat{u})\\
&\left.- 2g_{A\tilde{t}_1\tilde{t}_2}^2m_{\tilde{t}_1}^2\tilde{F}^{\tilde{t}_1\tilde{t}_2}(\hat{s},\hat{t},\hat{u}) + (\tilde{t}_1 \leftrightarrow \tilde{t}_2)\right\},
\end{aligned} \tag{B.37}$$

$$\begin{aligned}
F_{+-}^{\tilde{t}_1\tilde{t}_2} &= \frac{3e^2Q_t^2g_{A\tilde{t}_1\tilde{t}_2}^2}{8\pi^2 Y}\{\hat{s}(\hat{s}-2m_{\tilde{t}_1\tilde{t}_2}^2)C_0^{\tilde{t}_1\tilde{t}_1\tilde{t}_1}(\hat{s})\\
&+ (\hat{t}^2+\hat{u}^2-2m_A^4)C_{AA}^{\tilde{t}_1\tilde{t}_2\tilde{t}_1}(\hat{s})\\
&+ Y(m_{\tilde{t}_1}^2+m_{\tilde{t}_2}^2)D_{AA}^{\tilde{t}_1\tilde{t}_2\tilde{t}_2\tilde{t}_1}(\hat{t},\hat{u})\\
&+ \hat{s}(m_{\tilde{t}_1}^2-m_{\tilde{t}_2}^2)^2\tilde{F}^{\tilde{t}_1\tilde{t}_2}(\hat{s},\hat{t},\hat{u})\\
&- \hat{t}E_1^{\tilde{t}_1\tilde{t}_2}(\hat{s},\hat{t}) - \hat{u}E_1^{\tilde{t}_1\tilde{t}_2}(\hat{s},\hat{u})\\
&- 2(\hat{s}\hat{t}m_{\tilde{t}_2}^2+\hat{t}_1^2m_{\tilde{t}_1}^2)D_{AA}^{\tilde{t}_1\tilde{t}_2\tilde{t}_1\tilde{t}_1}(\hat{s},\hat{t})\\
&- 2(\hat{s}\hat{u}m_{\tilde{t}_2}^2+\hat{u}_1^2m_{\tilde{t}_1}^2)D_{AA}^{\tilde{t}_1\tilde{t}_2\tilde{t}_1\tilde{t}_1}(\hat{s},\hat{u}) + (\tilde{t}_1 \leftrightarrow \tilde{t}_2)\},
\end{aligned} \tag{B.38}$$

which involve contributions either from a single $\tilde{t}_j$ running along the loop, or mixed contributions involving both $\tilde{t}_1, \tilde{t}_2$. In (B.35)–(B.38) a factor 3 for color has already been introduced, while the necessary couplings are given by combining (A.20) and (A.21).

If other kinds of sfermions turn out also to be light, then their contribution can readily be derived from (B.35)–(B.38) by changing the appropriate couplings.

References

1. Opportunities and requirements for experimentation at a very high energy e^+e^- collider, SLAC-329(1928); Proceedings Workshops on Japan Linear Collider, KEK Reports, 90-2, 91-10 and 92-16; P.M. Zerwas, DESY 93-112, August 1993; Proceedings of the Workshop on e^+e^- Collisions at 500 GeV: The Physics Potential, DESY 92-123A,B(1992), C(1993), D(1994), E(1997), edited by P. Zerwas; E. Accomando et al., Phys. Rep. C **299**, 299 (1998)

2. V. Telnov, hep-ex/0003024; hep-ex/0001029; hep-ex/9802003; hep-ex/9805002; hep-ex/9908005; I.F. Ginzburg, hep-ph/9907549; R. Brinkman hep-ex/9707017
3. V. Telnov, talk at the International Workshop on High Energy Photon Colliders, 14–17 June 2000, DESY Hamburg, Germany, to appear in Nucl. Instr. and Meth. A
4. I.F. Ginzburg, G.L. Kotkin, V.G. Serbo, V.I. Telnov, Nucl. Instr. and Meth. **205**, 47 (1983); I.F. Ginzburg, G.L. Kotkin, V.G. Serbo, S.L. Panfil, V.I. Telnov, Nucl. Instr. and Meth. **219**, 5 (1984); J.H. Kühn, E. Mirkes, J. Steegborn, Z. f. Phys. C **57**, 615 (1993)
5. M. Baillargeon, G. Bélanger, F. Boudjema, talk given at Two-Photon Physics from DAPHNE to LEP200 and Beyond, Paris, France, 2–4 February 1994, edited by F. Kapusta, J. Parisi (World Scientific, Singapore) p. 267, hep-ph/9405359; hep-ph/9409263, Phys. Rev. D **51**, 4712 (1995); F. Boudjema, hep-ph/9809220
6. M. Krämer, J. Kühn, M.L. Stong, P.M. Zerwas, Z. f. Phys. C **64**, 21 (1994); G.J. Gounaris, J. Layssac, F.M. Renard, Z. f. Phys. C **65**, 245 (1995); G.J. Gounaris, F.M. Renard, Z. f. Phys. C **69**, 513 (1996); S.Y. Choi, K. Hagiwara, M.S. Baek, Phys. Rev. D **54**, 6703 (1996); G.J. Gounaris, G.P. Tsirigoti, Phys. Rev. D **56**, 3030 (1997); Phys. Rev. D **58**, 059901 (1998)
7. G.J. Gounaris, J. Layssac, F.M. Renard, Z. f. Phys. C **69**, 505 (1996); G.J. Gounaris, talk at Two-Photon Physics from DAPHNE to LEP200 and Beyond, Paris, France, 2–4 February 1994, edited by F. Kapusta, J. Parisi (World Scientific, Singapore) p. 243
8. G.J. Gounaris, D.T. Papadamou, F.M. Renard, Z. f. Phys. C **76**, 333 (1997); K. Hagiwara, S. Ishihara, R. Szalapski, D. Zeppenfeld, Phys. Rev. D **48**, 2182 (1992)
9. H. Nilles, Phys. Rep. **110**, 1 (1984); H.E. Haber, G.L. Kane, Phys. Rep. **117**, 75 (1985); J. Rosiek, Phys. Rev. D **41**, 3464 (1990), hep-ph/9511250(E); M. Kuroda, hep-ph/9902340
10. The minimal supersymmetric standard model: Group Summary Report, edited by A. Djouadi, S. Rosier-Lees et al., hep-ph/9901246; V. Barger et al., Report of SUGRA Working Group for Run II of the Tevatron, hep-ph/0003154
11. M.M. Mühlleitner, M. Krämer, M. Spira, P.M. Zerwas, talk at the International Workshop on High Energy Photon Colliders, 14–17 June 2000, DESY Hamburg, Germany, to appear in Nucl. Instr. and Meth. A; H.E. Haber et al., hep-ph/0007006
12. M. Spira, Fortsch. Phys. **46**, 203 (1998), hep-ph/9705337; M. Spira, P.M. Zerwas, hep-ph/9803257, Lectures at 36th Internationale Universitatswochen für Kernphysik und Teilchenphysik, Schladming, Austria, 1–8 March 1997
13. G.J. Gounaris, P.I. Porfyriadis, F.M. Renard, hep-ph/9812378, Phys. Lett. B **452**, 76 (1999); Phys. Lett. B **464**, 350 (1999) (E); G.J. Gounaris, P.I. Porfyriadis, F.M. Renard, hep-ph/9902230, Eur. Phys. J. C **9**, 673 (1999); G.J. Gounaris, J. Layssac, P.I. Porfyriadis, F.M. Renard, hep-ph/9904450, Eur. Phys. J. C **10**, 499 (1999)
14. G.J. Gounaris, J. Layssac, P.I. Porfyriadis, F.M. Renard, hep-ph/9909243, Eur. Phys. J. C **13**, 79 (2000)
15. G. Passarino, M. Veltman, Nucl. Phys. B **160**, 151 (1979)
16. G. Jikia, Nucl. Phys. B **412**, 57 (1994)
17. E.W.N. Glover, J.J. van der Bij, Nucl. Phys. B **309**, 282 (1988)
18. G. Jikia, Nucl. Phys. B **405**, 24 (1993)
19. M. Jacob, G.C. Wick, Ann. Phys. (N.Y.) **7**, 404 (1959)
20. S.H. Zhu, C.S. Li, C.S. Gao, Phys. Rev. D **58**, 015006 (1998)
21. A. Belyaev, M. Drees, O.J.P. Éboli, J.K. Mizukoshi, S.F. Novaes, Phys. Rev. D **60**, 075008 (1999); hep-ph/9910400
22. S. La-Zhen, L. Yao-Yang, Phys. Rev. D **54**, 3563 (1996)
23. S.H. Zhu, J. Phys. G **24**, 1703 (1998)
24. D.A. Dicus, C. Kao, Phys. Rev. D **49**, 1265 (1994)
25. S. Ambrosanio, G. Blair, P.M. Zerwas in DESY/ECFA 1998/99 LC Workshop. For more details, see http://www.hep.ph.rhbnc.ac.uk/blair/susy
26. G.J. van Oldenborgh, J.A.M. Vermaseren, Z. f. Phys. C **46**, 425 (1990); G.J. van Oldenborgh, FF: A package to evaluate one loop Feynman diagrams, Comput. Phys. Commun. **66**, 1 (1991)
27. V. Barger, T. Han, J. Jiang, hep-ph/0006223
28. See, e.g., H. Davoudiasl, Phys. Rev. D **60**, 084022 (1999); hep-ph/0001248; K. Cheung, Phys. Rev. D **61**, 015005 (2000); D. Atwood, S. Bar-Shalom, A. Soni, hep-ph/9906400; S.R. Choudhury, A. Cornell, G.C. Joshi, Phys. Lett. B **481**, 45 (2000), hep-ph/0001061
29. G.J. Gounaris, J. Layssac, F.M. Renard, hep-ph/0003143, to appear in Phys. Rev. D
30. A. Djouadi, J.L. Kneur, G. Moultaka, Nucl. Phys. B **569**, 53 (2000)
31. K. Hagiwara, S. Matsumoto, D. Haidt, C.S. Kim, Z. f. Phys. C **64**, 559 (1995)